



1 **Field measurements of methylglyoxal using Proton Transfer**
2 **Reaction-Time of Flight Mass Spectrometry and comparison**
3 **to the DNPH/HPLC-UV method**

4 Vincent Michoud^{1,2}, Stéphane Sauvage¹, Thierry Léonardis¹, Isabelle Fronval¹, Alexandre
5 Kukui³, Nadine Locoge¹, Sébastien Dusanter¹

6

7 [1] IMT Lille Douai, Univ. Lille, SAGE - Département Sciences de l'Atmosphère et Génie de
8 l'Environnement, 59000 Lille, France

9 [2] LISA/IPSL, Laboratoire Interuniversitaire des Systèmes Atmosphériques, UMR CNRS 7583,
10 Université Paris Est Créteil (UPEC) et Université Paris Diderot (UPD), Créteil, France

11 [3] Laboratoire de Physique et Chimie de l'Environnement et de l'Espace (LPC2E), UMR6115 CNRS-
12 Université d'Orléans, 45071 Orléans CEDEX 2, France

13

14 **Abstract**

15

16 Methylglyoxal (MGLY) is an important atmospheric α -dicarbonyl species whose
17 photolysis acts as a significant source of peroxy radicals, contributing to the oxidizing capacity
18 of the atmosphere and, as such, the formation of secondary pollutants such as organic aerosols
19 and ozone. However, despite its importance, only a few techniques exhibit time resolutions and
20 detection limits that are suitable for atmospheric measurements.

21 This study presents, to the best of our knowledge, the first measurements of ambient
22 MGLY using Proton Transfer Reaction-Time of Flight Mass Spectrometry (PTR-ToFMS).
23 These measurements were performed during the ChArMEx SOP2 field campaign. This
24 campaign took place at a Mediterranean site characterized by intense biogenic emissions and
25 low levels of anthropogenic trace gases. Concomitant measurements of MGLY were performed
26 using the 2,4-dinitrophenylhydrazine (DNPH) derivatization technique and High Performance
27 Liquid Chromatography (HPLC) with UV detection. PTR-ToFMS and DNPH-HPLC
28 measurements were compared to determine whether these techniques can perform reliable
29 measurements of MGLY.

30 Ambient time series revealed levels of MGLY ranging from 28-365 pptv, with a clear
31 diurnal cycle due to elevated concentrations of primary biogenic species during daytime, whose
32 oxidation led to large production rates of MGLY. A scatter plot of the PTR-ToFMS and DNPH-
33 HPLC measurements indicates a reasonable correlation ($R^2=0.48$) but a slope significantly



1 lower than unity (0.58 ± 0.05) and a significant intercept of 88.3 ± 8.0 pptv. A careful
2 investigation of the differences between the two techniques suggests that this disagreement is
3 not due to spectrometric interferences from $\text{H}_3\text{O}^+(\text{H}_2\text{O})_3$, MEK (or butanal) detected at m/z
4 73.050 and m/z 73.065 , respectively, which are close to the MGLY m/z of 73.029 . The
5 differences are more likely due to uncorrected sampling artefacts such as overestimated
6 collection efficiency or loss of MGLY into the sampling line for the DNPH-HPLC technique
7 or unknown isobaric interfering compounds such as acrylic acid and propanediol for the PTR-
8 ToFMS.

9 Calculations of MGLY loss rates with respect to OH-oxidation and direct photolysis
10 indicate similar contributions for these two loss pathways.

11

12 **1 Introduction**

13

14 Methylglyoxal (MGLY, $\text{CH}_3\text{C}(\text{O})\text{CHO}$) is an important α -dicarbonyl species in the
15 atmosphere. It is mainly produced during the oxidation of Volatile Organic Compounds (VOCs)
16 amongst which isoprene and acetone are the main contributors. Fu et al., (2008) calculated
17 production rates of 110 and 10 Tg year⁻¹ from the oxidation of isoprene and acetone,
18 respectively. Other precursors of MGLY are C_3 - C_5 isoalkanes (Jacob et al., 2002), aromatic
19 compounds (Volkamer et al., 2001; Pan and Wang, 2014; Wu et al., 2014)), and monoterpenes
20 (Fick et al., 2003; Nunes et al., 2005). Due to the anthropogenic and biogenic natures of MGLY
21 precursors, this compound can therefore be found in significant levels (low tens to hundreds of
22 pptv) in urban, rural or even remote and marine environments (Henry et al., 2012 and references
23 therein).

24 The principal sink of MGLY is thought to be photolysis (Fu et al., 2008), which can
25 significantly contribute to the formation of RO_x ($\text{OH} + \text{HO}_2 + \text{RO}_2$) radicals in the troposphere
26 (Dusanter et al., 2009), which in turn can enhance the formation rates of secondary pollutants,
27 including ozone and Secondary Organic Aerosol (SOA). In addition, MGLY has been identified
28 as a direct precursor of SOA (Altieri et al., 2008; Hallquist et al., 2009), due to aqueous
29 reactions in clouds leading to the formation of oligomers and oxalic acids, which can then form
30 SOA upon cloud droplet evaporation (Altieri et al., 2008).

31 Despite the important role of MGLY in the atmosphere, there are only a few measurement
32 techniques, most of them being expensive, requiring highly skilled operators, or suffering from
33 low time resolution. A common method relies on chemical derivatization and chromatographic



1 analysis. Several derivatization agents can be used to trap carbonyl compounds such as 2,4-
2 dinitrophenylhydrazine (DNPH) (Lee et al., 1998; Ho et al., 2014a; Lawson et al., 2015), o-(2,
3 3, 4, 5, 6-pentafluorobenzyl)hydroxylamine (PFBHA) (Spaulding et al., 1999; Ho and Yu,
4 2002; Ortiz et al., 2006, 2013; Temime et al., 2007) and pentafluorophenylhydrazine (PFPH)
5 (Ho and Yu, 2004; Pang and Lewis, 2011; Pang et al., 2011; Dai et al., 2012). Methods relying
6 on chemical derivatization imply active sampling through cartridges or liquid solutions
7 containing the selected reagent and a subsequent offline analysis using Gas Chromatography-
8 Mass Spectrometry (GC-MS) or High Performance Liquid Chromatography with ultraviolet
9 detection (HPLC-UV). Low detection limits are reached for these techniques with the
10 advantages of monitoring several carbonyl compounds simultaneously. Indeed, Ho and Yu
11 (2004) reported detection limits below 0.3 ppbv for a large range of carbonyl compounds,
12 including formaldehyde, acetaldehyde, propanal, acrolein, glyoxal, MGLY and others. These
13 authors used cartridges loaded with PFPH on a Tenax sorbent, a sampling time of 4 h and a
14 sampling flow rate of 100 mL min⁻¹. Ait-Helal et al. (2014) even reported lower detection limits
15 ranging from 10-60 pptv for C1-C9 aldehydes and ketones, including MGLY, using a sampling
16 duration of 3h for DNPH cartridges and a sampling flow rate of 1.5 L min⁻¹. The cartridges
17 were analysed by HPLC-UV. However, the main drawback of these methods is the low time
18 resolution of typically 3-4 h, which is too long to investigate photochemical processes.

19 Alternative techniques based on mist chambers and derivatization solutions such as
20 PFBHA (Spaulding et al., 2002) or DNPH (Munger et al., 1995) were used to measure MGLY
21 with a faster time resolution of approximately 10 min and low limits of detection (LOD).
22 Spaulding et al. (2002) reported a LOD of 7.7 pptv at a sampling flow rate of 25-70 L min⁻¹
23 (Spaulding et al., 2002). More recently, a microfluidic derivatization approach using PFBHA
24 and a planar glass micro-reactor was developed to measure glyoxal and MGLY at a time
25 resolution of 30 min and sampling flow rate ranging from 100 to 600 mL min⁻¹ (Pang et al.,
26 2014). This setup exhibits LODs of 76 and 185 pptv (3σ) for glyoxal and MGLY, respectively.
27 The authors also report the use of a Solid Phase MicroExtraction (SPME) method, previously
28 described by Gomez Alvarez et al. (2012), capable of measuring MGLY with a LOD of
29 150 pptv (3σ) and a measurement time of 25 min. The SPME technique relies on a derivatization
30 of aldehyde species into oximes on a fibre loaded with PFBHA and a subsequent analysis by
31 Gas Chromatography-Flame Ionization Detection (GC-FID). Gomez Alvarez et al. (2007) also
32 mentioned the possibility to measure MGLY using a SPME instrument as well as a Gas
33 Chromatography-Electron Capture Detector (GC-ECD), both calibrated against Fourier
34 Transform Infrared Spectroscopy (FTIR).



1 In addition to these chemical derivatization methods, optical/spectroscopic approaches
2 have also been employed to measure MGLY. Henry et al. (2012) reported a Laser-Induced
3 Phosphorescence (LIP) instrument capable of simultaneous measurements of glyoxal and
4 MGLY with a time resolution of 5 min and LODs of 4.4 and 243 pptv (3σ), respectively.
5 Thalman and Volkamer (2010) developed a blue LED (Light-Emitting Diodes) Cavity
6 Enhanced Differential Optical Absorption Spectroscopy (CE-DOAS) instrument for in-situ
7 measurements of MGLY among other compounds (nitrogen dioxide, glyoxal, iodine oxide and
8 water vapour). This instrument exhibits a LOD of 170 pptv (2σ) at a time resolution of 1 min.
9 Incoherent Broadband Cavity Enhanced Absorption Spectroscopy (IBBCEAS) has also been
10 used to measure both Glyoxal (Washenfelder et al., 2011) and MGLY (Pang et al., 2014), with
11 a LOD of 1 ppbv (3σ) for a measurement time of 20 s for the latter. FTIR is another
12 spectroscopic method capable of measuring MGLY (Talukdar et al., 2011). However, FTIR
13 exhibits a LOD in the ppbv range, which is not low enough for ambient measurements, even
14 with a long path length of hundreds of meters (Pang et al., 2014). Overall, while these
15 spectroscopic techniques usually exhibit performances that are suitable for atmospheric
16 measurements, they also require highly skilled operators and the use of fragile pieces of
17 equipment (light sources, mirrors etc...).

18 The use of Proton Transfer Reaction-Time of Flight Mass Spectrometry (PTR-ToFMS)
19 has been attempted for Glyoxal measurements by Stonner et al. (2017). However, these authors
20 showed that the sensitivity of PTR-ToFMS instruments was too low to monitor ambient
21 concentrations. MGLY measurements by PTR-ToFMS have been reported by Pang et al. (2014)
22 and Thalman et al. (2015) during intercomparison experiments. Pang et al. (2014) observed a
23 significant disagreement between PTR-ToFMS measurements and results from other
24 techniques (Microfluidic derivatization, IBBCEAS, FTIR, SPME) during photo-oxidation
25 experiments of isoprene under low NO_x conditions in the EUPHORE chamber. According to
26 the authors, this disagreement was due to interferences from $(\text{H}_2\text{O})_3\cdot\text{H}_3\text{O}^+$ at m/z 73 (no
27 deconvolution of peaks within this mass unit). Thalman et al. (2015) also reported interferences
28 from the $(\text{H}_2\text{O})_3\cdot\text{H}_3\text{O}^+$ cluster and the fragmentation of larger compounds upon protonation.
29 However, blank measurements made at the same relative humidity than in ambient air should
30 contain the contribution of $(\text{H}_2\text{O})_3\cdot\text{H}_3\text{O}^+$ and frequent blank measurements, as usually done
31 during field campaigns, could easily be subtracted to reduce the impact of $(\text{H}_2\text{O})_3\cdot\text{H}_3\text{O}^+$ on the
32 MGLY measurements. De Gouw and Warneke (2007) reported measurements of
33 methylethylketone (MEK) at the same unit mass using a PTR-MS equipped with a quadrupole.
34 However, Time of Flight mass spectrometers provide the opportunity to deconvolve signals of



1 MGLY (m/z 73.029) and MEK (m/z 73.065), which are separated by 0.036 Daltons. Thus, if
2 the mass resolution of the PTR-ToFMS instrument is sufficient, an adequate peak fitting
3 procedure and frequent blank measurements should allow a selective detection of
4 methylglyoxal.

5 In this study, we present online measurements of MGLY using Proton Transfer Reaction-
6 Time of Flight Mass Spectrometry (PTR-ToFMS). This study describes a procedure to conduct
7 measurements of MGLY using PTR-ToFMS, reports a comparison of PTR-ToFMS and DNPH-
8 HPLC measurements performed during an intensive field campaign in the Mediterranean basin,
9 and presents an investigation of the MGLY loss rate during this campaign.

10

11 **2 Experimental**

12

13 **2.1 The Chemistry-Aerosol Mediterranean Experiment (ChArMEx)**

14

15 The ChArMEx SOP2 (Short Observation Period 2) field campaign took place from 15
16 July to 05 August at Cape Corsica (France) on a hilltop (alt. 533 m) within a wind farm
17 (42.969°N, 9.380°E). It is a coastal site surrounded by the sea a few km away in all directions
18 (2.5-6 km) (Zannoni et al., 2015). The site was covered by typical Mediterranean vegetation
19 (“maquis” shrub-land) (Zannoni et al., 2015) leading to large emissions of biogenic VOCs and
20 elevated concentrations of isoprene (up to 1.3 ppbv) and monoterpenes (up to 2.2 ppbv)
21 (Michoud et al., 2017). Since MGLY is a byproduct of isoprene oxidation (2nd & 3rd
22 generations), this site is of interest to perform and investigate its budget. On the contrary, low
23 anthropogenic influence was observed at the measurement site since the closest city, Bastia, is
24 located ~30 km away (Michoud et al., 2017).

25

26 **2.2 PTR-ToFMS measurements**

27

28 Measurements of MGLY, among other species (Michoud et al., 2017), were conducted
29 using a PTR-ToFMS instrument from KORE IncTM (2nd generation). Ambient air was sampled
30 through a 5-m long line made of PFA (PerFluoroAlkoxy). The line was held at 50°C and the
31 flow rate was set at 1.2 L min⁻¹ to reduce the residence time below 4-s. The PTR-ToFMS
32 sampled from this line at a constant flow rate of 150 mL min⁻¹. Reactor pressure and temperature
33 were set at 1.33 mbar and 40°C, respectively, leading to an E/N value of 135 Td. The PTR-
34 ToFMS spectra were integrated over 10 minutes, leading to 6 measurements per hour.



1 An automatized zero procedure was performed for 10 minutes every hour to subtract
2 potential contaminations from the lines and to suppress interferences from water clusters and
3 other ions formed inside the glow discharge. Zero air was generated by passing ambient air
4 through a catalytic converter (1/2" stainless steel tubing filled with 2 grams of Pt wool held at
5 350°C) allowing to zero the instrument at the same relative humidity than in ambient air. In
6 order to test the efficiency of the catalytic converter, mixtures of several tens of hydrocarbons
7 at the ppb level were passed through the converter and the remaining VOCs were measured by
8 GC analyzers. Levels lower than the detection limits of the GCs (5-10 pptv) were observed,
9 indicating an efficient removal of the VOCs.

10 VOC signals were extracted from the 10-min mass spectra by summing the number of
11 counts detected within m/z windows centred on the exact masses of the VOCs of interest
12 ($m/z_{\text{VOC}} \pm 0.21$). These signals were normalized by the signals of H_3O^+ and the ionic water
13 cluster $\text{H}_3\text{O}^+(\text{H}_2\text{O})$ as proposed by de Gouw and Warneke (2007). VOC concentrations were
14 then calculated using Eq. 1.

$$[RH] = \frac{i_{RH_net}}{(i_{H_3O^+} \times 500 + X_r \cdot i_{H_3O^+(H_2O)} \times 250)} \cdot \frac{150000}{R_f} \quad (1)$$

15 Where i_{RH_net} is the net VOC signal (difference of signals recorded when sampling
16 ambient and zero air), $i_{H_3O^+}$ the signal from H_3O^+ ions at m/z 21, $i_{H_3O^+(H_2O)}$ the signal from
17 $\text{H}_3\text{O}^+(\text{H}_2\text{O})$ at m/z 39, X_r a factor to account for the effect of humidity on the PTR-ToFMS
18 sensitivity (de Gouw and Warneke, 2007), R_f the sensitivity determined by calibration (in
19 ncps ppb⁻¹) and 150000 the corresponding number of primary H_3O^+ ions in the PTR-ToFMS
20 reactor (in cps). The instrument was calibrated every three days during the campaign using a
21 Gas Calibration Unit (IONICON®) and various standards (RESTEK, PRAXAIR) made of
22 hydrocarbons (isoprene, benzene, toluene, o-xylene, ethylbenzene, α -pinene) and mono-
23 functional oxygenated VOCs (methanol, acetaldehyde, acetone, methylethylketone). These
24 calibrations were performed at a relative humidity of 50% at 20°C without passing by the entire
25 5-m long heated sampling line. X_r was determined by conducting additional calibrations at
26 various relative humidity values before and after the campaign. The calibration factor, R_f in Eq.
27 1, was normalized to 150000 cps of reagent ions. Specific calibrations performed for
28 methylglyoxal are described in section 3.1.

29 As mentioned in the introduction, MGLY and MEK are detected at m/z 73.029 and
30 73.065, respectively. A Gaussian peak fitting operation was performed to deconvolve the two
31 peaks observed in the m/z window 72.95-73.15 during ambient sampling, using the curvefit



1 tools from Grams™ software (Thermo Scientific™) (see supplementary material figure S1). The
2 signals recorded in this window were accumulated over 1 h to reduce the time needed for this
3 procedure, which was made manually. An automatic peak fitting operation is planned in the
4 future via the development of a software. The MEK-to-methylglyoxal ratio of areas observed
5 for the 1 h cumulated signals was then applied to each 10 min recorded signals (total number
6 of counts recorded within the m/z window 72.95-73.15) providing measurements of
7 methylglyoxal and MEK at a 10 min time resolution. It is worth noting that the MGLY lifetime
8 of at least 1 h and the longer lifetime of MEK ensure that the MGLY-to-MEK ratio does not
9 change significantly over an hour. Once the signals were deconvolved for each compound, the
10 procedure described in the previous paragraph was applied to calculate their ambient
11 concentrations using appropriate sensitivity and humidity dependence factors.

12 The 3σ detection limits were calculated from the hourly blank measurements. The
13 average detection limit for methylglyoxal during the whole campaign is 22 pptv (3σ) at the time
14 resolution of 10 min. The total uncertainty was estimated following the “Aerosols, Clouds, and
15 Trace gases Research InfraStructure network” guidelines (ACTRIS Measurement Guideline
16 VOC, 2012), taking into account precision and systematic errors. The repeatability on MGLY
17 measurements was calculated as the square root of the net signal (i_{RH_net}) since the statistic for
18 PTR-ToFMS signals follows a Poisson distribution (de Gouw and Warneke, 2007) and was on
19 average $9\pm 3\%$. The systematic errors concerned the calibration factor (R_f) and the peak fitting
20 procedure and are estimated to be 22% for methylglyoxal.

21

22 **2.3 Active sampling on DNPH cartridges**

23

24 Measurements of carbonyl compounds from C_1 to C_8 , including MGLY and MEK, were
25 performed using DNPH cartridges (Waters™) and an automatic sampler (ACROSS-TERA
26 Environment™), based on the US EPA TO-11A method. The analysis of the cartridges was
27 performed in the laboratory using HPLC-UV (Waters 2695 & 2487). This deployment has
28 already been described by Ait-Helal et al. (2014) and Michoud et al. (2017). Ambient air was
29 sampled through a 3-m long PFA line ($1/4''$) at a height of 1.5 m above the roof of the trailer
30 next to the PTR-ToFMS sampling line. This air was collected for 3 h on each cartridge at a flow
31 rate of 1.5 L min^{-1} . A potassium iodide (KI) ozone scrubber and a stainless steel particle filter
32 (porosity: $2\mu\text{m}$) were setup on the sampling line before the automatic sampler. The 3σ detection
33 limit was determined to be 6 pptv for MGLY from blank cartridges (unused cartridges stored



1 under similar conditions than exposed cartridges). The systematic error is estimated to be 25%
2 for these measurements.

3 The HPLC-UV instrument used to analyse the DNPH samples was calibrated using a
4 standard solution of hydrazone compounds (TO11/IP-6A) commercialized by SUPELCO.
5 However, MGLY-DNPH is not present in this solution and a hydrazone standard was made by
6 mixing a known volume of an aqueous solution of MGLY (40% in water, Acros Organics™)
7 into an excess of acidified DNPH solution. It is worth noting that calibrating the HPLC-UV
8 using a liquid standard of hydrazones is based on the assumption that the collection efficiency
9 of carbonyl compounds through DNPH cartridges is 100%.

10

11 **2.4 Investigation of the Methylglyoxal loss rate**

12

13 Two sinks were considered in the steady state loss calculations: reaction of MGLY with
14 OH and MGLY photolysis. The loss from the reaction with OH was calculated using
15 concentrations of both MGLY and OH, the latter being measured by Chemical Ionisation Mass
16 Spectrometry (Kukui et al. 2008), and the recommended rate constant of $1.50 \times 10^{11} \text{ cm}^3$
17 $\text{molecule}^{-1} \text{ s}^{-1}$ (Atkinson et al., 2006). $J(\text{NO}_2)$ and the photolysis frequencies for some other
18 species were derived from the actinic flux measured with an actinic flux spectroradiometer
19 METCON 6007 (Meteorologie Consult GmbH). However, Photolysis frequencies for MGLY
20 were not derived from these measurements. The approach described in Dusanter et al. (2009)
21 was therefore employed to calculate $J(\text{MGLY})$ and $J(\text{NO}_2)$ as a function of the solar zenith
22 angle for the measurement site (lat: 42.969°N , long: 9.380°E) using the Master Chemical
23 Mechanism (MCM) parameterization (Jenkin et al. 1997; Saunders et al., 2003). This
24 parameterization was derived for an ozone column of 345 Dobson, an altitude of 500 m and
25 clear sky conditions. Calculated values of $J(\text{MGLY})$ were then corrected for differences in
26 altitude, cloud covering, aerosol and O_3 column densities using a scaling factor derived from
27 the measured-to-calculated $J(\text{NO}_2)$ ratio. The photolytic loss of MGLY was calculated using
28 these scaled photolysis frequencies and PTR-ToFMS measurements of MGLY.

29

30 **3 Results and Discussion**

31

32 **3.1 PTR-ToFMS calibrations for MGLY**

33



1 These calibrations were not performed during the field campaign but a few months later
2 using a Liquid Calibration Unit (LCU, IONICON™) and an aqueous solution of MGLY (40%,
3 Acros Organics™) (see Figure 1). The LCU allows generating a standard mixture containing the
4 targeted compounds at known mixing ratios by evaporating an aqueous solution of these
5 compounds into a large flow of zero air (1.0 L min⁻¹ in our case). The standard solution flows
6 was varied between 1 and 20 μL min⁻¹ to generate MGLY concentrations ranging from 0.6 to
7 11 ppbV.

8 Figure 1 shows that the PTR-ToFMS response is linear with the MGLY concentration
9 over the tested range, with no significant offset. While the lower limit of the tested range is
10 larger than observed ambient concentrations (0.05-0.3 ppbv, figure 2), it has to be noted that
11 the PTR-MS response has always been observed to be linear with the analyte concentration and
12 a linear response is expected for MGLY for mixing ratios below 0.6 ppbv. These calibration
13 experiments indicate an averaged calibration factor of 2.54 ± 0.49 ncps ppb⁻¹ when normalized
14 to 150000 cps of reagent ions and using a Xr factor set to 0.5. It is worth noting that changing
15 the flow rate of the liquid standard solution to generate various MGLY concentrations leads to
16 a change in humidity in the gas exiting the LCU, tracked by the m/z 37-to-m/z 19 ratio (varying
17 from 0.1 to 0.5) during these calibration experiments. The good linearity observed in Fig. 1
18 gives confidence in the Xr factor value used to determine the calibration factor. Therefore, the
19 same Xr value of 0.5 was used for ambient measurements of MGLY.

20 To account for a potential drift in sensitivity between the field measurements and the
21 calibration experiments performed later in the laboratory, calibrations of MEK were also
22 performed during the laboratory experiments using a Gas Calibration Unit (GCU, IONICON™)
23 and a standard mixture provided by IONICON (Restek™). A comparison between MEK
24 response factors observed during field measurements and laboratory experiments allows
25 accounting for a drift of the PTRMS sensitivity as further discussed below. The Restek mixture
26 contains 15 compounds including 0.99 ± 0.05 (2σ) ppmv of MEK. Calibrations of MEK were
27 performed every 3 days during the field experiments using the GCU and the same Restek
28 mixture. Since MEK is detected at the same mass unit than MGLY, a change in sensitivity for
29 MGLY between the field measurements and the laboratory calibrations due to a change in ion
30 transmission inside the mass spectrometer would also be observed for MEK. A ratio of the
31 calibration factors measured for MGLY and MEK during the laboratory experiments was used
32 to calculate the MGLY calibration factor from the calibration factor measured for MEK during
33 the field campaign. The laboratory calibrations led to an averaged sensitivity factor of
34 6.60 ± 0.16 ncps ppb⁻¹ for MEK when normalized to 150000 cps of reagent ions, leading to a



1 MGLY-to-MEK sensitivity ratio of 0.38. During the ChArMEx field campaign, an averaged
2 calibration factor of 7.57 ± 0.52 ncps ppb⁻¹ was observed for MEK when normalized to 150000
3 cps of reagent ions, indicating a decrease of approximately 13% between the field and
4 laboratory measurements. However, as mentioned above, using the MGLY-to-MEK sensitivity
5 ratio determined in the laboratory allows correcting for this change.

6

7 **3.2 Time series of MGLY**

8

9 Concomitant measurements of MGLY by PTR-ToFMS and the DNPH/HPLC-UV
10 method in an environment characterized by intense biogenic emissions represent a good
11 opportunity to test how the two techniques compare for this compound. Figure 2 presents time
12 series of MGLY measurements from PTR-ToFMS (red) and active sampling on DNPH
13 cartridges (black) from 15 July to 6 August. The PTR-ToFMS measurements performed at a
14 time resolution of 10 min were averaged over 3 h around the sampling middle time of each
15 cartridge measurement to allow a direct comparison between the two techniques. This figure
16 shows that significant levels of MGLY were observed during the campaign, with concentrations
17 ranging from 30 to 370 pptv. In addition, these measurements indicate clear diurnal variations,
18 which is consistent with similar variations of MGLY precursors of biogenic origin observed
19 during the campaign, e.g. isoprene and monoterpenes (see Figure 2, middle panel). Figure 3
20 displays campaign averaged diurnal profiles for MGLY and indicates daily maxima observed
21 around 13:45 local time (Central European Summer Time +02:00 UTC) when the
22 photochemistry is the most intense (see Figure 2, bottom panel).

23

24 **3.3 Comparison of MGLY measurements**

25

26 Overall, a reasonable agreement is observed between the two techniques (see Figure 2),
27 except for 17 July, 25 July and the last 4 days where the measured PTR-ToFMS concentrations
28 were higher by 16-148%. A close look at Figure 2 also indicates that PTR-ToFMS
29 measurements are usually higher at night and the concentrations do not decrease as low as that
30 observed for the cartridges. For example, 3-h averaged PTR-ToFMS concentrations measured
31 at 1:30, 4:30 and 22:30 (local time) for the overall campaign (Figure 3) are 127, 144 and
32 136 pptv, respectively, which are approximately 14, 21 and 30 pptv higher (11-22%) than
33 cartridge measurements, respectively.



1 Figure 4 displays a scatter plot of PTR-ToFMS vs. DNPH/HPLC-UV measurements.
2 While a reasonable correlation is found between the two techniques ($R^2=0.48$), a significant
3 intercept of 88 ± 16 pptv (1σ) confirms the higher concentrations observed by PTR-ToFMS at
4 night, suggesting a positive offset on the PTR-ToFMS measurements, a negative offset on the
5 cartridge measurements or both. In contrast, a slope significantly lower than unity (0.58 ± 0.10 ,
6 1σ) seems to indicate a negative bias in the response of the PTR-ToFMS measurements, a
7 positive bias for the cartridge measurements or both.

8 A calibration issue cannot explain an intercept in the scatter plot but could explain part
9 of the disagreement observed for the slope. Three potential reasons may lead to a calibration
10 issue: (i) the generation of unreliable calibration standards, a humidity dependence of (ii) the
11 PTR-ToFMS response or (iii) the DNPH derivatization. The procedures used to calibrate the
12 PTR-ToFMS and the HPLC-UV are described in the experimental section. Two different
13 commercial methylglyoxal solutions were used to generate both the gas-phase standard for the
14 PTR-ToFMS and the liquid standard for the HPLC-UV. While we cannot rule out an issue with
15 the MGLY solutions, it seems unlikely that the disagreement between the two techniques is
16 only due to unreliable MGLY solutions since the good agreement observed on some days (21-
17 22, 27, 31 July and 1 August) contrasts with the bad agreement observed on other days (17 July,
18 2-5 August) when MGLY peaks during daytime (200-300 ppt).

19 As previously mentioned for the PTR-ToFMS calibration, varying the concentration of
20 MGLY in the range 0.6-11 ppbv with the LCU led to a change in RH. Calculating the calibration
21 factor at each concentration, i.e. at different RH, from the ratio of the measured normalized
22 signal-to-the MGLY concentration and plotting it as a function of the m/z 37-to- m/z 19 ratio
23 (Figure S2) does not indicate a significant water dependence of the PTR-ToFMS response. The
24 humidity dependence of the DNPH/HPLC-UV method has been recently investigated for some
25 ketone compounds, including acetone and MEK (Ho et al., 2014b). It was shown that the
26 collection efficiency is inversely related to relative humidity, with up to 35-80 % of the ketones
27 being lost for RH values higher than 50% at 22°C. While MGLY exhibits a ketone function it
28 also exhibits an aldehyde function and it is not clear whether this compound will behave as
29 simple ketones. The color coding shown in Figure 4 indicates that when higher RH values are
30 observed (60-100%), lower MGLY concentrations and larger relative differences between the
31 two techniques are also observed. Figure 5 displays a scatter plot of the difference between the
32 PTR-ToFMS and DNPH/HPLC-UV measurements and relative humidity, showing a weak
33 linear correlation with a negative slope. This trend with humidity seems to support that the
34 collection efficiency of MGLY on DNPH cartridges decreases with RH. It is interesting to note



1 that a collection efficiency lower than 100%, even at low RH values, may explain lower
2 concentrations measured by the DNPH/HPLC-UV method, on average, for the overall
3 campaign.

4 A positive or negative bias in the PTR-ToFMS measurements could be due to an
5 inadequate peak fitting procedure to separate the signals detected at m/z 73.029 (MGLY) and
6 m/z 73.065 (MEK + butanal) (see section 2.2). To check whether the peak fitting procedure can
7 lead to a bias in the measurements, Figure 5 also presents a scatter plot of the difference between
8 the PTR-ToFMS and DNPH/HPLC-UV measurements and the MEK+butanal concentration
9 measured by PTR-ToFMS. This scatter plot indicates a very weak correlation (R^2 of 0.05),
10 suggesting that the fitting procedure was able to deconvolute the signals from MGLY and
11 MEK+butanal. A weaker correlation is even found when the difference is plotted as a function
12 of butanal, which was measured by DNPH/HPLC-UV (see supplement S3).

13 An ionic water cluster, $(\text{H}_2\text{O})_3\cdot\text{H}_3\text{O}^+$, can also be detected at m/z 73.050. However, as
14 mentioned previously, the signal from this cluster is recorded during blank measurements and
15 subtracted from ambient measurements. As a consequence, the detection of $(\text{H}_2\text{O})_3\cdot\text{H}_3\text{O}^+$ at m/z
16 73 should not impact MGLY measurements reported in this study. Since the abundance of
17 $(\text{H}_2\text{O})_3\cdot\text{H}_3\text{O}^+$ is highly dependent on the ambient water concentration, relative humidity was
18 used as a proxy to investigate whether the cluster signal is efficiently recorded in the blank
19 signal, which was performed hourly to ensure that RH does not change significantly between
20 two blank measurements. A good correlation ($R^2=0.45\pm 0.21$, from daily analyses) observed
21 between the blank signal at m/z 73 with the m/z 37-to- m/z 19 ratio (proxy for humidity content),
22 indicates that the $(\text{H}_2\text{O})_3\cdot\text{H}_3\text{O}^+$ water cluster signal is indeed recorded during blank
23 measurements.

24 Scatter plots of the difference between PTR-ToFMS and DNPH/HPLC-UV
25 measurements with O_3 , acetaldehyde and nopinone were generated (see supplement S3) to
26 check whether the possible secondary formation of isobaric OVOCs (malondialdehyde, acrylic
27 acid) in the atmosphere, from the oxidation of ambient VOCs, or in the sampling line from
28 reaction of O_3 with unsaturated compounds adsorbed on surfaces, could lead to a positive bias
29 in the PTR-ToFMS measurements. The very weak correlations (R^2 of 0.02, 0.01 and <0.01 for
30 O_3 , acetaldehyde and nopinone, respectively) observed in Figure S3 rule out this possibility.

31 Similar correlation plots were made for m/z 137 (monoterpenes), 139 (Nopinone), 151
32 (Pinonaldehyde) and 155 (unidentified oxidation product of monoterpenes) measured by PTR-
33 ToFMS (see supplement S4) to track whether differences observed between both techniques
34 could be explained by interferences from the fragmentation of larger compounds observed at



1 significant concentrations during the CharMEx field campaign. Poor correlations were found
2 ($R^2 < 0.06$) suggesting that MGLY measurements were free of interferences from the
3 fragmentation of compounds measured at these four masses. Nevertheless, we cannot rule out
4 interferences from the fragmentation of other higher m/z compounds.

5 A closer look at the blank signals measured at m/z 73 shows that this signal correlates
6 with the total m/z 73 signal on some days (21-22/07, 26-27/07, 01-03/08), with R^2 factors
7 ranging from 0.36-0.56. Lower correlations are observed on other days ($R^2 < 0.20$). Interestingly,
8 a scatter plot between the coefficients of determination for the above mentioned correlations
9 and the daily averaged relative humidity exhibits an anti-correlation (negative slope, $R^2 = 0.58$)
10 (see supplement S5). This type of correlation has also been observed by de Gouw et al. (2003),
11 who explained this behaviour by the sticky nature of MGLY, which could cause a memory
12 effect in the sampling lines. Different sampling line lengths and characteristics (heated at 50°C
13 for PTR-ToFMS and not heated for DNPH cartridges, presence of a stainless steel particle filter
14 and a KI ozone scrubber for DNPH cartridges) could lead to different artefacts related to
15 adsorption or heterogeneous reaction on line surfaces for the two techniques. It is worth noting
16 that performing blank measurements every hour and the use of a high flow rate and heated
17 sampling line likely reduces this artefact for the PTR-ToFMS, while blank measurements for
18 DNPH cartridges only takes into account passive contamination of the cartridges, without any
19 artefact from lines considered. It is interesting to note that while the difference between the two
20 techniques is not correlated to the PTR-ToFMS measurements (see supplement S3), a fair
21 correlation ($R^2 = 0.35$) is observed with the cartridge measurements, which may suggest a bias
22 on the cartridge measurements.

23 While a reasonable agreement is observed between the 2 techniques, a close look at the
24 correlation between the two measurement sets indicates that the DNPH/HPLC-UV methods
25 measured lower concentrations than the PTR-ToFMS technique by 18% on average. The above
26 discussion highlights several potential reasons for this disagreement: (i) calibration standards
27 of MGLY are difficult to generate for both techniques and require further work to straighten
28 out this aspect, (ii) the impact of artefacts from sampling lines needs to be further investigated
29 to evaluate their significance, (iii) the collection efficiency of MGLY in DNPH cartridges needs
30 to be investigated under ambient sampling conditions to assess whether MGLY is completely
31 collected and whether there is a humidity dependence.

32 Finally, we cannot exclude that differences observed between PTR-ToFMS and
33 DNPH/HPLC-UV measurements of MGLY are partly due to differences in sampling sequences
34 (3h continuous sampling for DNPH/HPLC-UV, 3h sampling minus 3 times ten minutes of blank



1 measurements for PTR-ToFMS). However, the impact of differences in timescale for the two
2 techniques should lead to random scatter when the measurements are compared and not to a
3 systematic difference as observed in this study.

4

5 **3.4 MGLY loss rate**

6

7 Loss rates of MGLY are presented in Figure 6. They were calculated as described in
8 section 2.4 using PTR-ToFMS measurements since the DNPH/HPLC-UV measurements may
9 suffer from inlet effects and an overestimated collection efficiency. The total loss rate peaks
10 during daytime around 14:00 local time at values ranging from 100-350 pptv h⁻¹. The calculated
11 loss rate is almost equally divided into photolysis and oxidation by OH, accounting for 53%
12 and 47%, respectively, of the average diurnal loss from 10:00 to 19:00 local time.

13 A thorough investigation of the MGLY budget would require calculating the total
14 MGLY production rate from the oxidation of ambient VOCs for comparison to the total loss
15 rate presented above. However, as mentioned in the introduction, MGLY is produced during
16 the oxidation of many VOCs (isoprene, monoterpenes, acetone, aromatics...) at average yields
17 which are strongly dependent on ambient radical concentrations and NO_x as recently reported
18 for isoprene [Jenkin et al., 2015]. It is also worth noting that calculating MGLY production
19 rates based on ambient concentrations of precursors and average yield values would only be
20 robust for first-generation oxidation products since no intermediate species is taken into
21 account. Taking into account that MGLY is also a second and higher generation oxidation
22 product in most degradation mechanisms would lead to a delayed formation. Indeed, MGLY
23 production can take hours in NO rich environments and even days in low NO_x environments
24 such as this study (Fu et al., 2008). As a consequence, it would be hazardous to try to calculate
25 local MGLY production rates from the measured VOC precursors.

26 When a gaseous species exhibits a lifetime lower than a few seconds/minutes, such as
27 radical species or highly photolabile compounds, this species should reach a photostationary
28 state and chemical production and loss rates should balance each other since transport processes
29 such as advection and vertical dilution are too slow to significantly impact the local
30 concentration of these short-lived species. MGLY exhibits a lifetime of approximately 1-2 h
31 during daytime, which may be short enough for the photostationary state to hold. In this case,
32 production rates of MGLY should mimic the loss rate displayed in Figure 6. However,
33 Washenfelder et al. (2011) showed a breakdown of the photostationary state when applied to
34 glyoxal, a dicarbonyl compound exhibiting a similar lifetime than MGLY, and as a consequence



1 the calculated loss rate reported in this study only provides a rough estimation of the local
2 production rate.

3

4 **4 Conclusions and discussion**

5

6 To the best of our knowledge, this study presents the first ambient measurements of
7 methylglyoxal by PTR-ToFMS. This work aims at describing a simple and proper procedure to
8 perform reliable measurements, relying on (i) the data processing proposed by de Gouw and
9 Warneke (2007) to account for the impact of ambient humidity on the PTR-ToFMS sensitivity,
10 (ii) automatized blank measurements performed every hour to suppress potential memory
11 effects and interferences from water clusters, and (iii) a gaussian peak fitting analysis to
12 deconvolute the methylglyoxal signal from other compounds exhibiting a similar mass unit but
13 different exact masses (i.e. butanone and butanal).

14 The ChArMEx SOP2 field campaign was conducted in an environment characterized
15 by high biogenic emissions, including isoprene, at the extreme north of the Corsica Island. This
16 campaign therefore provides a good opportunity to study methylglyoxal measurements, since
17 this compound is mainly formed via isoprene oxidation. Furthermore, concomitant
18 measurements of methylglyoxal by PTR-ToFMS and DNPH/HPLC-UV allowed an
19 intercomparison of these two techniques to test their reliability.

20 Time series of methylglyoxal measured by both PTR-ToFMS and DNPH/HPLC-UV
21 revealed concentration levels ranging from 28-365 pptv with a clear diurnal cycle due to the
22 secondary nature of this compound. The visual comparison of the measured time series shows
23 a reasonable agreement, with the DNPH/HPLC-UV methods measuring concentrations lower
24 by 18% on average compared to the PTR-ToFMS technique. A linear regression analysis
25 performed between the two measurement sets indicates a fair correlation with a determination
26 coefficient (R^2) of 0.48, a slope significantly different than unity (0.58 ± 0.10 , 1σ) and a non-
27 zero intercept (88.3 ± 15.9 pptv, 1σ). Interferences from $(\text{H}_2\text{O})_3 \cdot \text{H}_3\text{O}^+$, butanone and butanal can
28 be excluded for the PTR-ToFMS measurements, validating the procedure used for data
29 acquisition and analysis. Methylglyoxal formation into sampling lines due to heterogeneous
30 reactions of O_3 with adsorbed organic compounds is also not likely. Potential remaining
31 uncorrected artefacts from lines on some days for both techniques could be partly responsible
32 for measurements disagreements and this aspect needs to be further investigated to evaluate its
33 significance. In addition, this work questions the collection efficiency of MGLY in DNPH
34 cartridges, recommending to investigate it under ambient sampling conditions to assess whether



1 all the MGLY is collected and whether humidity dependence exists. Comparisons of PTR-
2 ToFMS with other existing techniques in the field and/or in atmospheric simulation chambers
3 would be of interest to identify potential artefacts causing the disagreement observed in this
4 study. Nevertheless, PTR-ToFMS seems promising for methylglyoxal measurements.

5 The methylglyoxal loss rate was studied at cape Corsica, revealing that the contributions
6 of direct photolysis and OH-oxidation were almost similar.

7
8

9 **Acknowledgement**

10
11

12 This study received financial support from Mistrals / ChArMEx programmes, ADEME,
13 the French environmental ministry, and the CaPPA projects. The CaPPA project (Chemical and
14 Physical Properties of the Atmosphere) is funded by the French National Research Agency
15 (ANR) through the PIA (Programme d'Investissement d'Avenir) under contract "ANR-11-
16 LABX-0005-01" and by the Regional Council Nord-Pas de Calais and the "European Funds for
17 Regional Economic Development" (FEDER). This research was also funded by the European
18 Union Seventh Framework Programme under Grant Agreement number 293897, "DEFIVOC"
19 project and CARBOSOR/Primequal. This study also received funding from the Région Hauts-
20 de-France, the Ministère de l'Enseignement Supérieur et de la Recherche and the European
21 Fund for Regional Economic Development through the CLIMIBIO project.

22 The authors also want to thank Eric Hamonou and François Dulac for logistic
23 management during the campaign as well as all the participants of the ChArMEx SOP2 field
24 campaign.

25

26 **References**

27 ACTRIS Measurement Guidelines VOC, WP4-NA4: Trace gases networking: Volatile organic
28 carbon and nitrogen oxides Deliverable D4.1: Draft for standardized operating procedures
29 (SOPs) for VOC measurements, [http://ebas-](http://ebas-submit.nilu.no/Portals/117/media/SOPs/MG_VOC_draft_20120718.pdf)
30 [submit.nilu.no/Portals/117/media/SOPs/MG_VOC_draft_20120718.pdf](http://ebas-submit.nilu.no/Portals/117/media/SOPs/MG_VOC_draft_20120718.pdf), p: 24-32, 2012.

31 Ait-Helal, W., Borbon, A., Sauvage, S., de Gouw, J. A., Colomb, A., Gros, V., Freutel, F.,
32 Crippa, M., Afif, C., Baltensperger, U., Beekmann, M., Doussin, J.-F., Durand-Jolibois, R.,
33 Fronval, I., Grand, N., Leonardis, T., Lopez, M., Michoud, V., Miet, K., Perrier, S.,
34 Prévôt, A. S. H., Schneider, J., Siour, G., Zapf, P., and Locoge, N.: Volatile and intermediate



- 1 volatility organic compounds in suburban Paris: variability, origin and importance for SOA
2 formation, *Atmos. Chem. Phys.*, 14, 10439–10464, doi:10.5194/acp-14-10439-2014, 2014
- 3 Altieri, K. E., Seitzinger, S. P., Carlton, A. G., Turpin, B. J., Klein, G. C., and Marshall, A. G.:
4 Oligomers formed through in-cloud methylglyoxal reactions: Chemical composition,
5 properties, and mechanisms investigated by ultra-high resolution FT-ICR mass spectrometry,
6 *Atmos. Environ.*, 42, 1476–1490, doi:10.1016/j.atmosenv.2007.11.015, 2008.
- 7 Atkinson, R.: Gas-phase tropospheric chemistry of organic compounds: a review, *Atmos.*
8 *Environ.*, 41, S200–S240, 2007.
- 9 Atkinson, R., Baulch, D. L., Cox, R. A., Crowley, J. N., Hampson, R. F., Hynes, R. G., Jenkin,
10 M. E., Rossi, M. J., Troe, J., and IUPAC Subcommittee: Evaluated kinetic and photochemical
11 data for atmospheric chemistry: Volume II - gas phase reactions of organic species, *Atmos.*
12 *Chem. Phys.*, 6, 3625–4055, 2006.
- 13 Dai, W. T., Ho, S. S. H., Ho, K. F., Liu, W. D., Cao, J. J., and Lee, S. C.: Seasonal and diurnal
14 variations of mono- and di-carbonyls in Xi'an, China, *Atmos. Res.*, 113, 102–112, 2012.
- 15 de Gouw, J. and Warneke, C.: Measurements of volatile organic compounds in the earth's
16 atmosphere using proton-transfer reaction mass spectrometry, *Mass. Spectrom. Rev.*, 26, 223–
17 257, doi:10.1002/mas.20119, 2007.
- 18 de Gouw, J. A., Goldan, P. D., Warneke, C., Kuster, W. C., Roberts, J. M., Marchewka, M.,
19 Bertman, S. B., Pszenny, A. A. P., and Keene, W. C.: Validation of proton transfer reaction-
20 mass spectrometry (PTR-MS) measurements of gas-phase organic compounds in the
21 atmosphere during the New England Air Quality Study (NEAQS) in 2002, *J. Geophys. Res.*,
22 108, 4682, doi:10.1029/2003JD003863, 2003.
- 23 Dusanter, S., Vimal, D., Stevens, P. S., Volkamer, R., Molina, L. T., Baker, A., Meinardi, S.,
24 Blake, D., Sheehy, P., Merten, A., Zhang, R., Zheng, J., Fortner, E. C., Junkermann, W., Dubey,
25 M., Rahn, T., Eichinger, B., Lewandowski, P., Prueger, J., and Holder, H.: Measure- 15 ments
26 of OH and HO₂ concentrations during the MCMA-2006 field campaign – Part 2: Model
27 comparison and radical budget, *Atmos. Chem. Phys.*, 9, 6655–6675, doi:10.5194/acp-9- 6655-
28 2009, 2009.
- 29 Fick, J., Pommer, L., Nilsson, C., and Andersson, B.: Effect of OH radicals, relative humidity,
30 and time on the composition of the products formed in the ozonolysis of alpha-pinene, *Atmos.*
31 *Environ.*, 37, 4087–4096, 2003.
- 32 Fu, T.-M., Jacob, D. J., Wittrock, F., Burrows, J. P., Vrekoussis, M., and Henze, D. K.: Global
33 budgets of atmospheric glyoxal and methylglyoxal, and implications for formation of secondary
34 organic aerosols, *J. Geophys. Res.*, 113, D15303, doi:10.1029/2007JD009505, 2008.
- 35 Gómez Alvarez, E., Viidanoja, J., Muñoz, A., Wirtz, A., and Hjorth, J.: Experimental
36 confirmation of the dicarbonyl route in the photo-oxidation of toluene and benzene, *Environ.*
37 *Sci. Technol.*, 41, 8362–8369, doi:10.1021/es0713274, 2007.
- 38 Gomez Alvarez, E., Moreno, M. V., Gligorovski, S., Wortham, H., and Cases, M. V. R.:
39 Characterisation and calibration of active sampling Solid Phase Microextraction applied to
40 sensitive determination of gaseous carbonyls, *Talanta*, 88, 252–258, 2012.



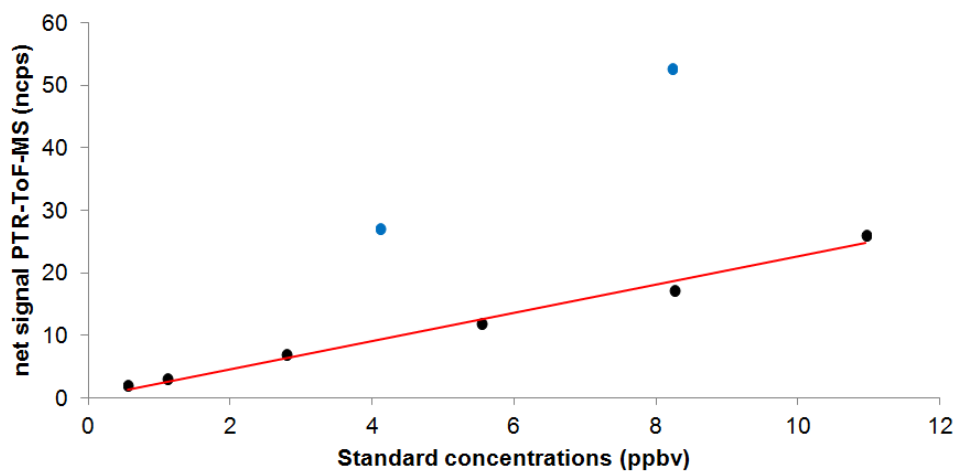
- 1 Hallquist, M., Wenger, J. C., Baltensperger, U., Rudich, Y., Simpson, D., Claeys, M., Dommen,
2 J., Donahue, N. M., George, C., Goldstein, A. H., Hamilton, J. F., Herrmann, H., Hoffmann, T.,
3 Iinuma, Y., Jang, M., Jenkin, M. E., Jimenez, J. L., Kiendler-Scharr, A., Maenhaut, W.,
4 McFiggans, G., Mentel, Th. F., Monod, A., Prévôt, A. S. H., Seinfeld, J. H., Surratt, J. D.,
5 Szmigielski, R., and Wildt, J.: The formation, properties and impact of secondary organic
6 aerosol: current and emerging issues, *Atmos. Chem. Phys.*, 9, 5155–5236, doi:10.5194/acp-9-
7 5155-2009, 2009.
- 8 Henry, S. B., Kammrath, A., and Keutsch, F. N.: Quantification of gas-phase glyoxal and
9 methylglyoxal via the LaserInduced Phosphorescence of (methyl)GLyOxal Spectrometry
10 (LIPGLOS) Method, *Atmos. Meas. Tech.*, 5, 181–192, doi:10.5194/amt-5-181-2012, 2012.
- 11 Ho, S. S. H. and Yu, J. Z.: Feasibility of Collection and Analysis of Airborne Carbonyls by On-
12 Sorbent Derivatisation and Thermal Desorption, *Anal. Chem.*, 74, 1232–1240, 2002.
- 13 Ho, S. S. H. and Yu, J. Z.: Determination of Airborne Carbonyls: Comparison of a Thermal
14 Desorption/GC Method with the Standard DNPH/HPLC Method, *Environ. Sci. Technol.*, 38,
15 862–870, 2004
- 16 Ho, K. F.; Ho, S.; Dai, W. T.; Cao, J. J.; Huang, R.-J.; Tian, L.; Deng, W. J.: Seasonal Variations
17 of Monocarbonyl and Dicarboxyl in Urban and Sub-Urban Sites of Xi'an, China, *Environ.*
18 *Monit. Assess.*, 186, 2835–2849, 2014a
- 19 Ho, S. S. H., Chow, J. C., Watson, J. G., Ip, H. S. S., Ho, K. F., Dai, W. T., and Cao, J.: Biases
20 in ketone measurements using DNPHcoated solid sorbent cartridges, *Analytical Methods*, 6,
21 967–974, doi:10.1039/C3AY41636D, 2014b
- 22 Jacob, D. J., Field, B. D., Jin, E., Bey, I., Li, Q., Logan, J., Yantosca, R. M. and Singh, H. B.:
23 Atmospheric budget of acetone, *J. Geophys. Res.-Atmos.*, 107, doi:10.1029/2001JD000694,
24 2002.
- 25 Jenkin, M. E., Saunders, S. M., and Pilling, M. J.: The tropospheric degradation of volatile
26 organic compounds: A protocol for mechanism development, *Atmos. Env.*, 31, 81–104, 1997.
- 27 Jenkin, M. E., Young, J. C., and Rickard, A. R.: The MCM v3.3.1 degradation scheme for
28 isoprene, *Atmos. Chem. Phys.*, 15, 11433-11459, <https://doi.org/10.5194/acp-15-11433-2015>,
29 2015.
- 30 Kukui, A., Ancellet, G., and Le Bras, G.: Chemical ionisation mass spectrometer for
31 measurements of OH and Peroxy radical concentrations in moderately polluted atmospheres, *J.*
32 *Atmos. Chem.*, 61, 133-154, 2008.
- 33 Lawson, S. J., Selleck, P. W., Galbally, I. E., Keywood, M. D., Harvey, M. J., Lerot, C.,
34 Helmig, D., and Ristovski, Z.: Seasonal in situ observations of glyoxal and methylglyoxal over
35 the temperate oceans of the Southern Hemisphere, *Atmos. Chem. Phys.*, 15, 223-240,
36 doi:10.5194/acp-15-223-2015, 2015.
- 37 Lee, Y. N., Zhou, X., Kleinman, L. I., Nunnermacker, L. J., Springston, S. R., Daum, P. H.,
38 Newman, L., Keigley, W. G., Holdren, M. W., Spicer, C. W., Young, V., Fu, B., Parrish, D. D.,
39 Holloway, J., Williams, J., Roberts, J. M., Ryerson, T. B., and Fehsenfeld, F. C.: Atmospheric
40 chemistry and distribution of formaldehyde and several multioxygenated carbonyl compounds



- 1 during the 1995 Nashville Middle Tennessee Ozone Study, *J. Geophys. Res.-Atmos.*, 103,
2 22449–22462, doi:10.1029/98jd01251, 1998.
- 3 Michoud, V., Sciare, J., Sauvage, S., Dusanter, S., Léonardis, T., Gros, V., Kalogridis, C.,
4 Zannoni, N., Féron, A., Petit, J.-E., Crenn, V., Baisnée, D., Sarda-Estève, R., Bonnaire, N.,
5 Marchand, N., DeWitt, H. L., Pey, J., Colomb, A., Gheusi, F., Szidat, S., Stavroulas, I., Borbon,
6 A., and Locoge, N.: Organic carbon at a remote site of the western Mediterranean Basin: sources
7 and chemistry during the ChArMEx SOP2 field experiment, *Atmos. Chem. Phys.*, 17, 8837–
8 8865, <https://doi.org/10.5194/acp-17-8837-2017>, 2017.
- 9 Munger, J. W., Jacob, D. J., Daube, B. C., Horowitz, L. W., Keene, W. C., and Heikes, B. G.:
10 Formaldehyde, glyoxal, and methylglyoxal in air and cloudwater at a rural mountain site in
11 central Virginia, *J. Geophys. Res. Atmos.*, 100, 9325–9333, 1995.
- 12 Nunes, F. M. N., Veloso, M. C. C., Pereira, P. A. D. P., and de Andrade, J. B.: Gas-phase
13 ozonolysis of the monoterpenoids (S)- (+)-carvone, (R)-(-)-carvone, (-)-carveol, geraniol and
14 citral, *Atmos. Environ.*, 39, 7715–7730, 2005.
- 15 Ortiz, R., Hagino, H., Sekiguchi, K., Wang, Q. Y., and Sakamoto, K.: Ambient air
16 measurements of six bifunctional carbonyls in a suburban area, *Atmos. Res.*, 82, 709–718,
17 doi:10.1016/j.atmosres.2006.02.025, 2006.
- 18 Ortiz, R., Shimada, S., Sekiguchi, K., Wang, Q., Sakamoto, K., Measurements of changes in
19 the atmospheric partitioning of bifunctional carbonyls near a road in a suburban area, *Atmos.*
20 *Environ.*, 81, 554–560, 2013.
- 21 Pan, S. S. and Wang, L. M.: Atmospheric Oxidation Mechanism of m-Xylene Initiated by OH
22 Radical, *J. Phys. Chem. A*, 118, 45, 10778–10787, doi:10.1021/jp506815v, 2014
- 23 Pang, X. and Lewis, A. C.: Carbonyl compounds in gas and particle phases of mainstream
24 cigarette smoke, *Sci. Total Environ.*, 409, 5000–5009, 2011.
- 25 Pang, X., Lewis, A. C., and Hamilton, J. F.: Determination of airborne carbonyls via
26 pentafluorophenylhydrazine derivatisation by GC-MS and its comparison with HPLC method,
27 *Talanta*, 85, 406–414, 2011.
- 28 Pang, X., Lewis, A. C., Rickard, A. R., Baeza-Romero, M. T., Adams, T. J., Ball, S. M., Daniels,
29 M. J. S., Goodall, I. C. A., Monks, P. S., Peppe, S., Ródenas García, M., Sánchez, P., and
30 Muñoz, A.: A smog chamber comparison of a microfluidic derivatisation measurement of gas-
31 phase glyoxal and methylglyoxal with other analytical techniques, *Atmos. Meas. Tech.*, 7, 373–
32 389, doi:10.5194/amt-7-373-2014, 2014.
- 33 Pope, C. A. and Dockery, D. W.: Health effects of fine particulate air pollution: Lines that
34 connect, *J. Air Waste Manage. Assoc.*, 56, 709–742, 2006.
- 35 Saunders, S. M., Jenkin, M. E., Derwent, R. G., and Pilling, M. J.: Protocol for the development
36 of the Master Chemical Mechanism, MCM v3 (Part A): Tropospheric degradation of
37 nonaromatic volatile organic compounds, *Atmos. Chem. Phys.*, 3, 161–180, 2003.
- 38 Spaulding, R. S., Frazey, P. A., Rao, X., and Charles, M. J.: Measurement of Hydroxy
39 Carbonyls and Other Carbonyls in Ambient Air Using Pentafluorobenzyl Alcohol as a
40 Chemical Ionization Reagent, *Anal. Chem.*, 71, 3420–3427, 1999.

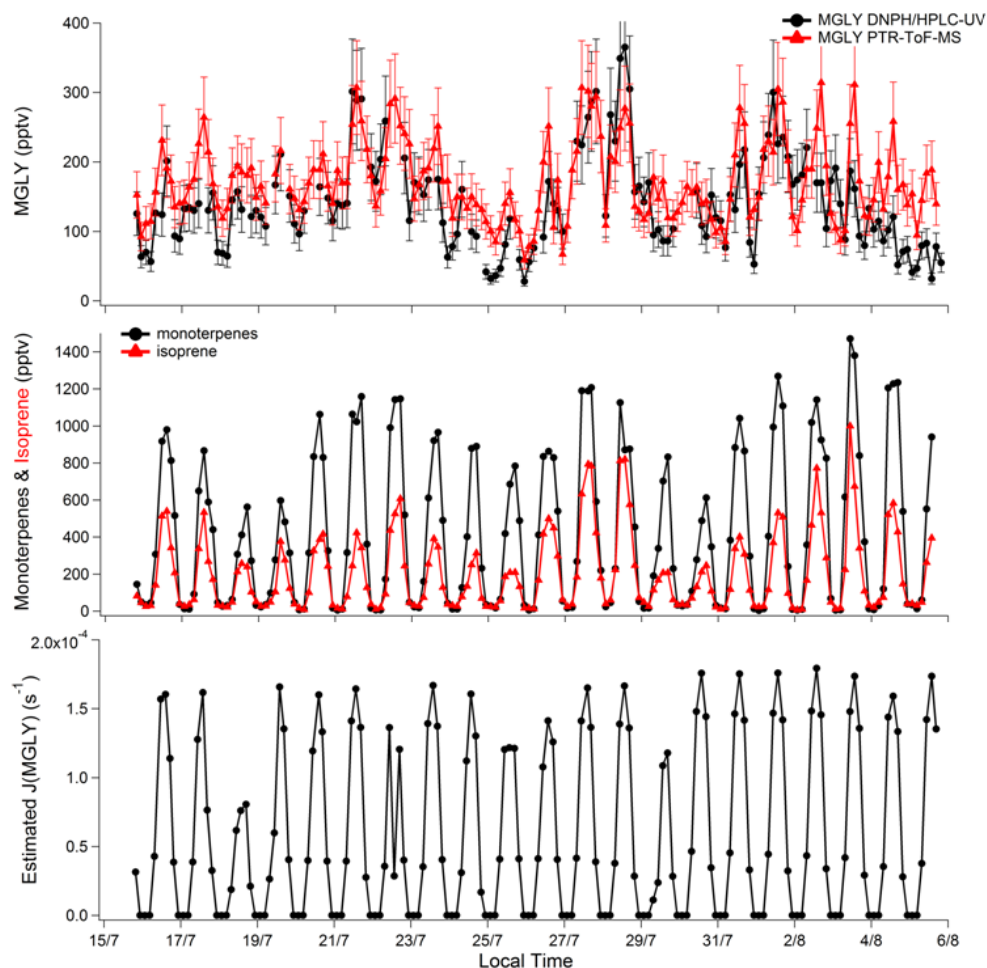


- 1 Spaulding, R. S., Talbot, R. W., and Charles, M. J.: Optimisation of a Mist Chamber (Cofer
2 Scrubber) for Sampling Water-Soluble Organics in Air, *Environ. Sci. Technol.*, 36, 1798–1808,
3 2002.
- 4 Stönnner, C., Derstroff, B., Klüpfel, T., Crowley, J., N., Williams, J.: Glyoxal measurement with
5 a proton transfer reaction time of flight mass spectrometer (PTR-TOF-MS): characterization
6 and calibration, *J. Mass Spectrom.*, 52, 30-35, 2017
- 7 Talukdar, R. K., Zhu, L., Feierabend, K. J., and Burkholder, J. B.: Rate coefficients for the
8 reaction of methylglyoxal (CH₃COCHO) with OH and NO₃ and glyoxal (HCO)₂ with NO₃,
9 *Atmos. Chem. Phys.*, 11, 10837–10851, doi:10.5194/acp-11-10837-2011, 2011.
- 10 Temime, B., Healy, R. M., and Wenger, J. C.: A Denuder-Filter Sampling Technique for the
11 Detection of Gas and Particle Phase Carbonyl Compounds, *Environ. Sci. Technol.*, 41, 6514–
12 6520, 2007.
- 13 Thalman, R. and Volkamer, R.: Inherent calibration of a blue LED-CE-DOAS instrument to
14 measure iodine oxide, glyoxal, methyl glyoxal, nitrogen dioxide, water vapour and aerosol
15 extinction in open cavity mode, *Atmos. Meas. Tech.*, 3, 1797–1814, doi:10.5194/amt-3-1797-
16 2010, 2010.
- 17 Thalman, R., Baeza-Romero, M. T., Ball, S. M., Borrás, E., Daniels, M. J. S., Goodall, I. C. A.,
18 Henry, S. B., Karl, T., Keutsch, F. N., Kim, S., Mak, J., Monks, P. S., Muñoz, A., Orlando, J.,
19 Peppe, S., Rickard, A. R., Ródenas, M., Sánchez, P., Seco, R., Su, L., Tyndall, G., Vázquez, M.,
20 Vera, T., Waxman, E., and Volkamer, R.: Instrument intercomparison of glyoxal, methyl
21 glyoxal and NO₂ under simulated atmospheric conditions, *Atmos. Meas. Tech.*, 8, 1835-1862,
22 doi:10.5194/amt-8-1835-2015, 2015.
- 23 Volkamer, R., Platt, U., and Wirtz, K.: Primary and secondary glyoxal formation from
24 aromatics: Experimental evidence for the bicycloalkyl-radical pathway from benzene, toluene,
25 and p-xylene, *J. Phys. Chem. A*, 105, 7865–7874, doi:10.1021/Jp010152w, 2001.
- 26 Washenfelder, R. A., Young, C. J., Brown, S. S., Angevine, W. M., Atlas, E. L., Blake, D. R.,
27 Bon, D. M., Cubison, M. J., de Gouw, J. A., Dusanter, S., Flynn, J., Gilman, J. B., Graus, M.,
28 Griffith, S., Grossberg, N., Hayes, P. L., Jimenez, J. L., Kuster, W. C., Lefer, B. L., Pollack, I.
29 B., Ryerson, T. B., Stark, H., Stevens, P. S., and Trainer, M. K.: The glyoxal budget and its
30 contribution to organic aerosol for Los Angeles, California, during CalNex 2010, *J. Geophys.*
31 *Res.*, 116, D00V02, doi:10.1029/2011JD016314, 2011.
- 32 Wu, R. R., Pan, S. S., Li, Y., Wang, L. M.: Atmospheric Oxidation Mechanism of Toluene, *J.*
33 *Phys. Chem. A*, 118, 25, 4533-4547, doi:10.1021/jp500077f, 2014
- 34 Zannoni, N., Dusanter, S., Gros, V., Sarda Esteve, R., Michoud, V., Sinha, V., Locoge, N., and
35 Bonsang, B.: Intercomparison of two Comparative Reactivity Method instruments in the
36 Mediterranean basin during summer 2013, *Atmos. Meas. Tech. Discuss.*, 8, 5065-5104,
37 doi:10.5194/amtd-8-5065-2015, 2015.



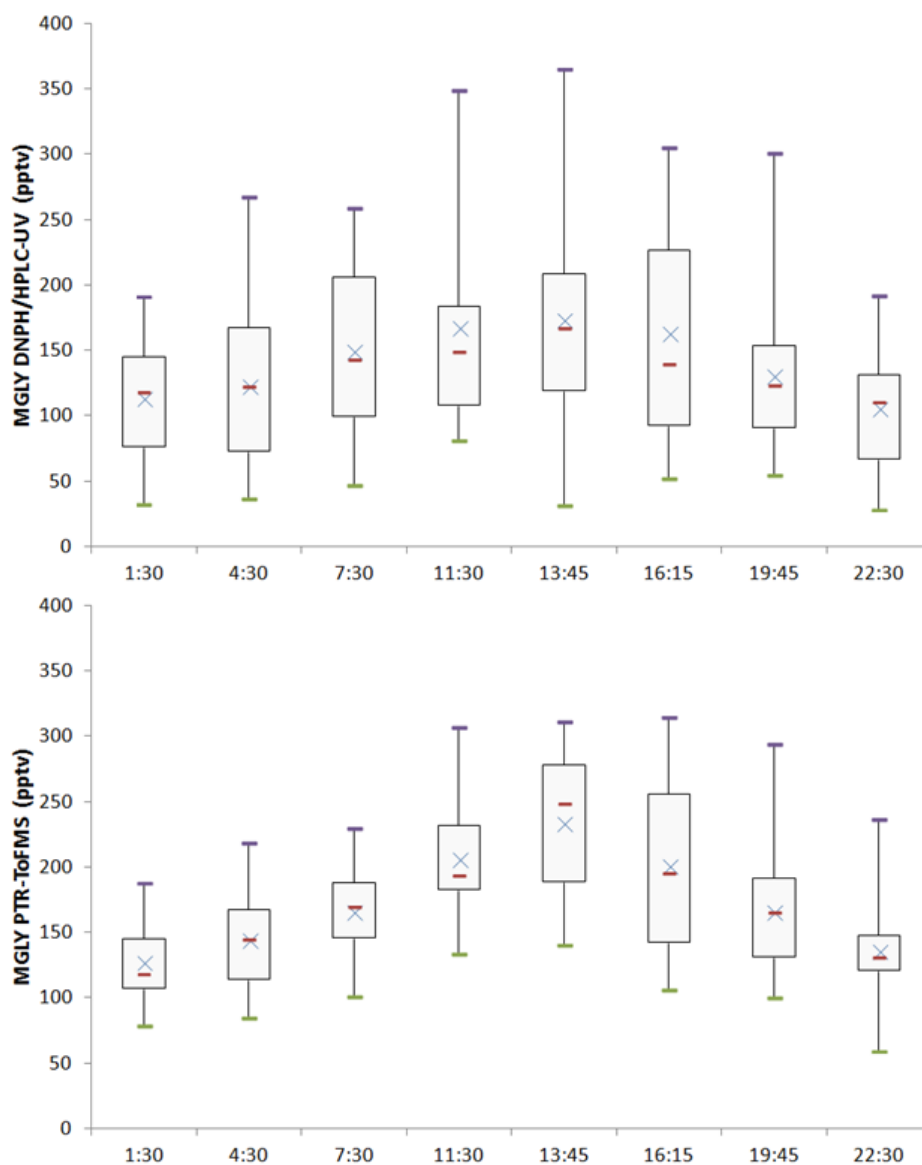
1

2 Figure 1: MGLY (black circles) and MEK (blue circles) calibration plot for PTR-ToFMS
3 measurements: normalized net signals at m/z 73.029 (MGLY, ncps) and 73.065 (MEK, ncps)
4 vs. generated mixing ratio (ppbv).



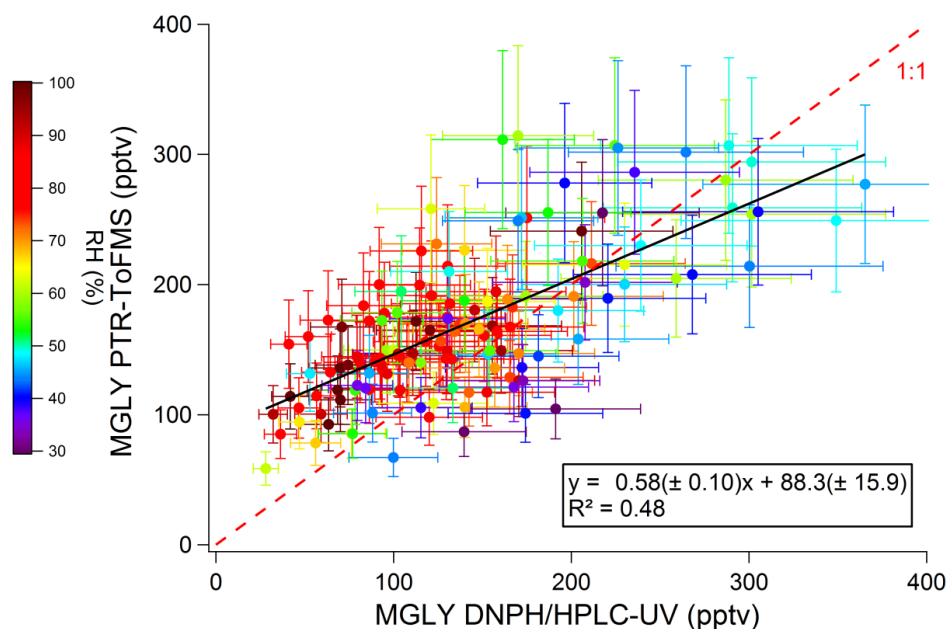
1

2 Figure 2 : Time series of MGLY measured by PTR-ToFMS (red) and active sampling on DNP
 3 cartridges (black) (top panel); sum of monoterpenes (black) and isoprene (red) measured by
 4 PTR-ToFMS (middle panel); and estimated $J(\text{MGLY})$ (black, bottom panel). Error bars for
 5 MGLY measurements (top panel) correspond to systematic errors of 22% and 25% for PTR-
 6 ToFMS and DNP cartridge measurements, respectively.



1

2 Figure 3: Diurnal profiles (Boxplots) of MGLY measured by both PTR-ToFMS (bottom panel)
3 and active sampling on DNP-HPLC-UV (top panel) for the campaign average. Purple bars
4 represent the maxima, green bars the minima, red bars the medians, blue crosses the averages,
5 and the sides of the boxes: the first (bottom) and the third (top) quartiles.

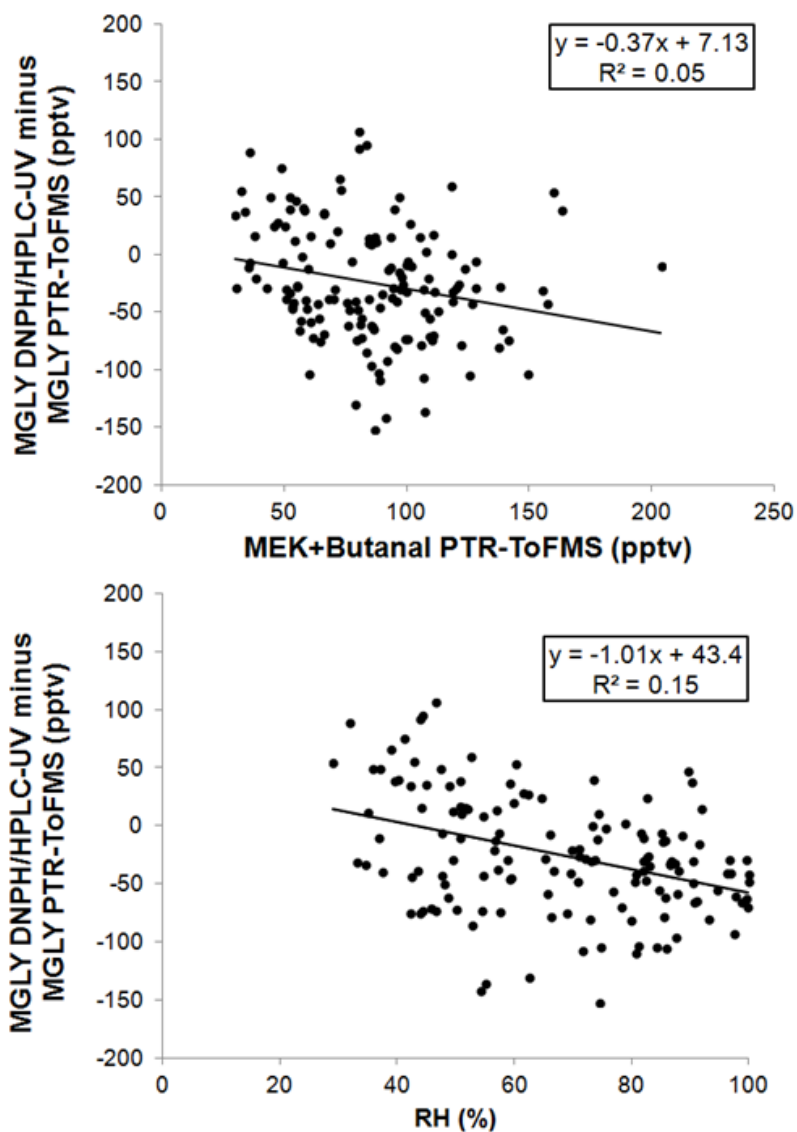


1

2 Figure 4: Scatter plot of MGLY concentrations measured by PTR-ToFMS versus
 3 concentrations measured by active sampling on DNP-H cartridges. Black line and insert
 4 represent the linear regression. Systematic errors associated to the PTR-ToFMS (22%) and
 5 DNP-H cartridge (25%) measurements are accounted for in the regression analysis. The scatter
 6 plot has been color-coded according to the relative humidity.

7

8

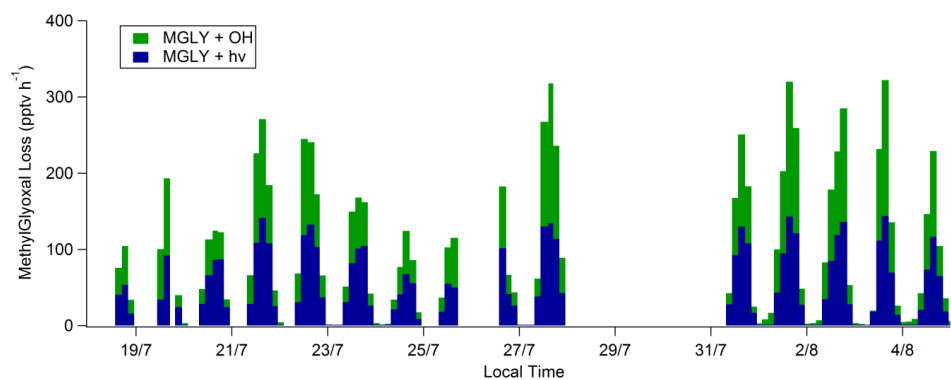


1

2 Figure 5 : Scatter plots of the difference between the two techniques and MEK+butanal (top
3 panel) or relative humidity (RH, bottom panel).

4

5



1

2 Figure 6: Time series of MGLY loss rates (pptv h⁻¹) from photolysis and reaction with OH.

3